MOLECULAR ECOLOGY

Molecular Ecology (2009) **18**, 3831–3846 doi: 10.1111/j.1365-294X.2009.04330.x

The effect of landscape features on population genetic structure in Yunnan snub-nosed monkeys (*Rhinopithecus bieti*) implies an anthropogenic genetic discontinuity

ZHIJIN LIU,* BAOPING REN,* RUIDONG WU,†‡ LIANG ZHAO,*§¶ YANLI HAO,*§ BOSHI WANG,*§ FUWEN WEI,* YONGCHENG LONG† and MING LI*

**Key Lab of Animal Ecology and Conservation Biology, Institute of Zoology, Chinese Academy of Sciences, 1 Beichen West Road, Chaoyang District, Beijing 100101, China, †China Program, The Nature Conservancy (TNC), The Building of the Yunnan Provincial Meteorological Bureau, 8th Floor, 77 Xichang Road, Kunming, Yunnan 650034, China, ‡College of Life Science, South China Normal University, Guangzhou, Guangdong 510631, China, §Graduate School of the Chinese Academy of Sciences, Beijing 100039, China, ¶Faculty of Biology, Suzhou University, Suzhou, Anhui 234000, China*

Abstract

The Tibetan Plateau is one of the top 10 biodiversity hotspots in the world and acts as a modern harbour for many rare species because of its relatively pristine state. In this article, we report a landscape genetic study on the Yunnan snub-nosed monkey (*Rhinopithecus bieti*), a primate endemic to the Tibetan Plateau. DNA was extracted from blood, tissue and fecal samples of 135 wild individuals representing 11 out of 15 extant monkey groups. Ten microsatellite loci were used to characterize patterns of genetic diversity. The most striking feature of the population structure is the presence of five subpopulations with distinct genetic backgrounds and unique spatial regions. The population structure of *R. bieti* appears to be shaped by anthropogenic landscape features as gene flow between subpopulations is strongly impeded by arable land, highways and human habitation. A partial Mantel test showed that 36.23% ($r = 0.51$, $P = 0.01$) of the genetic distance was explained by habitat gaps after controlling for the effect of geographical distance. Only 4.92% of the genetic distance was explained by geographical distance in the partial Mantel test, and no significant correlation was found. Estimation of population structure history indicates that environmental change during the last glacial maximum and human impacts since the Holocene, or a combination of both, have shaped the observed population structure of *R. bieti*. Increasing human activity on the Plateau, especially that resulting in habitat fragmentation, is becoming an important factor in shaping the genetic structure and evolutionary potential of species inhabiting this key ecosystem.

Keywords: anthropogenic genetic discontinuity, conservation, landscape genetics, microsatellite loci, *Rhinopithecus bieti*, Tibetan Plateau

Received 29 December 2008; revision received 4 July 2009; accepted 7 July 2009

Introduction

The Tibetan Plateau covers an area of 2.5 million km^2 and has an average height above sea level of 4500 m. It is the loftiest and most immense massif on Earth and sometimes referred to as 'the third polar region' (Zhang *et al.* 2002). The continuing uplift of the plateau is because of the India–Asia tectonic collision which began in the Early Miocene (Patriat & Achache 1984). The Tibetan Plateau is regarded one of the top 10 biodiversity hotpots in the world because of its high biodiversity and number of unique endemic species (Hewitt 2000; Myers *et al.* 2000). For example, a total of 12 000 species of vascular plants, 210 mammals, 532 birds and 115 fish have been recorded on the plateau (Wu & Feng

Correspondence: Ming Li, Fax: 8610-64807099;
E-mail: lim@ioz.ac.cn

1992). The topographic variation caused by Tibetan Plateau uplift and concomitant climate change are widely regarded as two of the most important factors influencing patterns of genetic diversity in wildlife inhabiting this region (Macey *et al.* 1998; Yu *et al.* 2004; Luo *et al.* 2004; Ruan *et al.* 2005; Qu *et al.* 2005, 2006; Liu *et al.* 2006; Peng *et al.* 2006; Zhang & Jiang 2006).

Although the plateau acts as a modern harbour for many rare species because of its high elevation and natural state, local species are being influenced by human activity (Wu & Feng 1992; Cincotta *et al.* 2000). The impact of the Qinghai–Tibet railway on the migration of Tibetan wild animals has become a public debate and received considerable interest (Brumfiel 2008). According to field surveys and direct observation, wild animals can migrate across the railway through designated underpasses (Yang & Xia 2008). However, there have been few population genetic studies to quantify the impact of human-made landscapes on gene flow and genetic diversity of local wild animals in this important part of the world.

In this article, we report landscape genetic analyses for Yunnan snub-nosed monkeys (*Rhinopithecus bieti*), a primate endemic to the Tibetan Plateau. Landscape genetics, an amalgamation of population genetics and landscape ecology, aims to provide information on how landscape and environmental factors influence gene flow and population structure (Manel *et al.* 2003). *Rhinopithecus bieti* is a good candidate for testing the impact of landscape and environmental factors on genetic patterns because of its close association with forest habitat. At present, *R. bieti* is confined to the high altitude forests 3000–4500 m above sea level on Yunling Mountain, within a narrow area between the Yangtze and Mekong rivers (98º37′–99º41′E, 26º14′–29º20′N), Yunnan Province, China. *Rhinopithecus bieti* is therefore the highest altitude-dwelling nonhuman primate (Long *et al.* 1996; Li *et al.* 2002). Recent surveys have revealed that the population comprises ~1500 individuals across 15 wild groups inhabiting fragmented forest patches (Long *et al.* 1996; Xiao *et al.* 2003). For reasons of its small population size, reduction in habitat, fragmentation and hunting threats, *R. bieti* was regarded one of the top 25 most endangered primates in the world (19th Congress of the International Primatological Society, Beijing, 2002).

Research on population genetics of *R. bieti* was sparse prior to our first large scale phylogeographic and genetic analysis using mitochondrial DNA (mtDNA) (Liu *et al.* 2007). MtDNA analysis revealed a moderate level of genetic diversity in *R. bieti*, and disaffirmed the hypothesis that *R. bieti* was a taxon with very low genetic variation. Moreover, mtDNA haplotypes in *R. bieti* displayed local homogeneity and strong population structure, implying limited gene flow between wild groups (Liu *et al.* 2007). Population structure and gene flow can be influenced by multiple factors. For example, in addition to habitat fragmentation, female philopatry in *R. bieti* would contribute to local homogeneity of mtDNA haplotypes. As mtDNA is a matrilineal molecular marker and cannot reflect gene flow in both sexes, a comprehensive population genetic study should include nuclear molecular markers inherited from both parents. Our goal here is to describe the population structure of *R. bieti* using 10 nuclear microsatellite loci and quantify the effect of human-made landscapes on population structure and gene flow using genetic analyses and landscape data. Understanding the population structure of this threatened species is crucial to developing a conservation plan (Lande & Barrowclough 1987; Simberloff 1988; Hanski & Gilpin 1997). Determining which groups are in contact will highlight important dispersal corridors and identify priority areas for conservation.

Materials and methods

Sample collection

Samples were collected from 11 of 15 extant monkey groups (G1–G15) across its entire range (Fig. 1a). *Rhinopithecus bieti* blood samples were collected opportunistically while attaching radio collars for another study. Muscle samples from dead individuals found in the wild were obtained and stored in 95% ethanol. Fecal samples from monkey groups in their respective patches were collected during direct behavioural observations, and stored in 95% ethanol. To initially avoid re-sampling of fecal samples from the same individual we sampled a group once on a certain day only, each dropping was identified by size, shape and colour, and multiple samples located <1.5 m apart were not collected (Hayaishi & Kawamoto 2006). Molecular markers were used to identify fecal samples and are described below.

Polymerase chain reaction amplification and genotyping

Genomic DNA was extracted from blood and tissue using SDS-phenol/chloroform (Sambrook *et al.* 1989). The QIAamp DNA Stool Mini Kit (QIAGEN GMBH) was used for fecal samples according to the manufacturer's protocol. Extraction blanks were used as negative controls in downstream polymerase chain reaction (PCR) amplifications. First, we tested these DNA extractions through PCR using mtDNA primers (Liu *et al.* 2007). DNA extractions from which mtDNA could be amplified successfully were then used for subsequent microsatellite loci amplification. Ten fluorescently labelled microsatellite loci (D1S533, D5S1457,

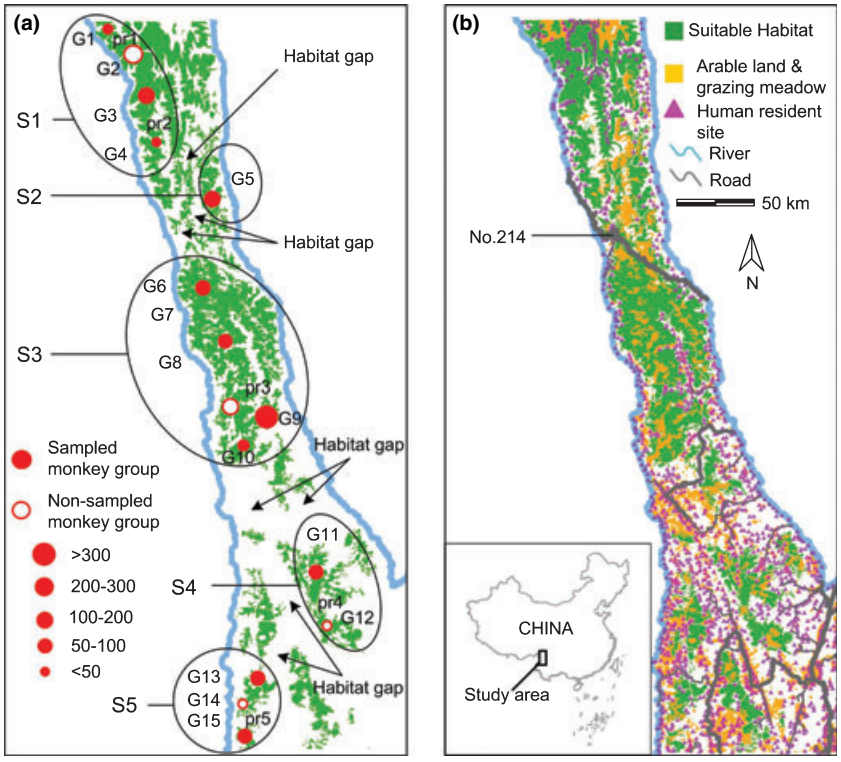

Fig. 1 Map of sampled groups and landscape features. (a) Map of suitable habitat for *Rhinopithecus bieti* and sampled groups. (b) Map of suitable habitat of *R. bieti*, arable land, grazing meadow, roads and human resident sites. Green area indicates suitable habitat that includes coniferous forests and mixed coniferous/broadleaf forests, while non-habitat includes arable land and grazing meadow (yellow areas), main roads and alleys (grey lines) and human resident sites (purple triangles).

D6S493, D8S505, D11S2002, D17S1290, GM108, GM109, GM209 and GM214) (Hao *et al.* 2007; Liu *et al.* 2008) were amplified using a multiple-tube procedure. In practice, DNA yields were such that most homozygote genotypes were confirmed by a minimum of seven replicates, and all heterozygotes were observed in a minimum of two separate reactions (Taberlet *et al.* 1996; Taberlet & Luikart 1999; Zhan *et al.* 2006). PCR products were electrophoresed on an ABI 3700 genetic analyser and alleles were sized using GENESCAN software (Applied Biosystems). The rate of genotyping error was calculated as the proportion of cases in which errors were detected vs. the total consensus genotypes following Creel *et al.* (2003). Microsatellite variation was assessed by summary statistics, including mean number of alleles per locus, expected (H_E) and observed (H_O) heterozygosity and inbreeding coefficient (F_{IS}), all obtained using GENETIX (Belkhir 2004). Linkage disequilibrium (LD) was estimated across all pairs of loci using the correlation coefficient of Weir (1979). A permutation approach was used to determine which LD values were significant. Allelic richness, an estimate of allelic diversity that compensates for unequal sample size, was calculated using FSTAT (Goudet 2002) and averaged across loci. Deviations from Hardy–Weinberg equilibrium for each population were assessed using an exact test implemented in GENEPOP 3.4 (Raymond & Rousset 2003).

Population structure analysis

First, genetic differentiation between sampled groups was assessed using traditional *F*-statistics (Wright 1978). *F*-statistics across the study area and between pairs of sampling sites were calculated using the estimator θ of Wright's F_{ST} (Weir & Cockerham 1984) by the program GENEPOP (Raymond & Rousset 2003). Significance values over all loci were obtained using a Fisher's exact test (Ryman & Jorde 2001) with 10 000 dememorization steps, 100 batches and 500 iterations per batch in the Markov chain method of Guo & Thompson (1992). Second, the software Structure 2.0 (Pritchard *et al.* 2000) was used to detect cryptic population genetic structure and assign individuals to inferred subpopulation clusters based on multilocus genotypes. Ten independent runs of K = 1–11 were performed at 2 000 000 Markov Chain Monte Carlo (MCMC) repetitions and a 200 000 burn-in period using no prior information and assuming correlated allele frequencies and admixture. K was identified using the maximal values of ln $P(D)$ (the posterior probability of the data for a given K) returned by Structure and ΔK based on the rate of change in the log probability of data between successive K-values (Evanno *et al.* 2005). The program also calculated the fractional membership of each individual in each cluster (Q). Parameter sets of the different Structure runs for specific goals are shown in Table S1.

Landscape genetics analysis

To visualize the spatial distribution of landscapes, we collected SPOT5 satellite imagery of the year 2005 (China Remote Sensing Satellite Ground Station) and developed a vegetation-mapping model with the software ARCGIS (Environmental Systems Research Institute). Coniferous forests and mixed coniferous/broadleaf forests were identified as suitable habitat for *R. bieti* (Long *et al.* 1994; Jablonski 1993; Kirkpatrick 1995). Main roads, alleys, arable land, grazing meadows and human villages and towns were also indicated on the landscape map and considered as habitat gaps. GENELAND version 1.0.5 (Guillot *et al.* 2005), a computer package in R 2.3.1 (Ihaka & Gentleman 1996), was used to verify our definition of *R. bieti* populations and locate areas of genetic discontinuity. Based on geo-referenced individual multilocus genotype data, GENELAND infers the most likely number of populations (*K*) in a data set. Additionally, areas of genetic discontinuity were also detected as geographical areas of global low posterior probability of population membership using GENELAND. First, we ran five independent MCMC chains for $K = 1$–11 (1 000 000 generations; sampling every 100; 10% generations burn-in), using the spatial Dirichlet-model as a prior for all allele frequencies. The maximum rate of the Poisson process was set to 135, with no uncertainty in the spatial coordinates, and the maximum number of nuclei in the Poisson–Voronoi tessellation was set to 405. Second, we ran the model to have it assign each individual to one of the *K* genetic groups. We performed another five independent runs using the parameter set established in the first step, with the most likely number of populations (*K*) inferred hereinbefore. Individuals in the same group were assigned to the same longitude and dimensionality coordinates. Detailed parameter settings of different runs are listed in Table S2.

Analysis of isolation by distance and isolation by barrier

Mantel tests (Mantel 1967) were performed to test the significance of regression between pairwise genetic distances expressed as $F_{ST}/(1 - F_{ST})$ against the natural geographical distance (Rousset 1997). To estimate the effect of the habitat gaps to gene flow, a categorical matrix was generated describing whether the sampling sites were on the same (=0) or different (=1) side of the habitat gap. Then this matrix was used in further Mantel tests to determine weather it co-varied with genetic distance (Lampert *et al.* 2003). Habitat gaps and geographical distance were not independent, because monkey groups separated by habitat gaps were usually farther apart from each other. Thus, a partial Mantel test (Smouse *et al.* 1986) was also performed to assess how much genetic differentiation could be attributed to a barrier after controlling for the effect of geographical distance. The Mantel test and partial Mantel test were performed using Arlequin 3.0 (Excoffier *et al.* 2005) and 10 000 iterations were used to determine the statistical significance of the results.

Calculation of migration rate and detection of migrant and admixed individuals

Migration rate between subpopulations was assessed using the software BAYESASS (Wilson & Rannala 2003). Detection of first generation migrants and admixed individuals was performed using Structure 2.0 and GENECLASS 2.0 (Cornuet *et al.* 1999). The use of prior population information allowed Structure to calculate posterior probabilities for which individuals belonged to their sampled locality/cluster. Therefore, Structure was run in this way with the previously inferred Structure cluster memberships ($K = 5$ from clustering analysis without population information) used as prior population information with MIGPRIOR = 0.005, which is the average level migration rate from BAYESASS (Wilson & Rannala 2003). Burn-in and run lengths were the same as runs without prior population information. The 'Detect first generation migrants' function in GENECLASS 2.0 was selected as it is designed explicitly to identify first generation migrants (Paetkau *et al.* 2004; Piry *et al.* 2004). L_h was used as the likelihood of finding a given individual in the population in which it was sampled and is the most appropriate statistic to use when all potential source populations have not been sampled (Paetkau *et al.* 2004; Piry *et al.* 2004). In addition, L_h/L_{max}, the ratio of L_h to the greatest likelihood among all sampled populations (Paetkau *et al.* 2004) was used, which has greater power and is most informative when all source populations have been sampled. We also performed an exclusion test (Cornuet *et al.* 1999) in GENECLASS 2.0 using population simulations to test statistically whether one or more of the subpopulations could be ruled out as the area of origin for each individual. The probability of individual genotypes coming from each subpopulation was calculated by comparing individual genotypes to 10 000 simulated individuals per locality. We selected the simulation method introduced by Paetkau *et al.* (2004) as it is more representative of real population processes than other methods (e.g. Rannala & Mountain 1997; Cornuet *et al.* 1999) which have been shown to produce an inflated rate of type I errors (Paetkau *et al.* 2004; Piry *et al.* 2004).

Analysis of population structure evolution and population demographic history

To assess when the observed population structure emerged, the data for selected pairs of subpopulations were also considered within an isolation with migration model that explicitly incorporates parameters for the time of population splitting, bidirectional gene flow after splitting, and population sizes, including the size of the ancestral population (Nielsen & Wakeley 2001; Hey & Nielsen 2004). The model fits a Bayesian framework that provides estimates for the posterior probability density of the model parameters, given the data (using the IM computer program and assuming a stepwise mutation model (SMM); Hey & Nielsen 2004). We used the program IM (5 March 2007 release; Hey 2006) for the MCMC estimation of posterior probability distributions of m_1 (=m_1/μ), m_2 (=m_2/μ), θ_1 (=$4N_1\mu$), θ_2 (=$4N_2\mu$), θ_A (=$4N_A\mu$), and t (=$t\mu$) corresponding to the migration rate between two populations, the current effective population size of two populations, the ancestral population size and the divergence time. IM analyses were run for each subpopulation pairwise comparison with a combined dataset of all microsatellite loci. To obtain demographic parameters, we assumed a mutation rate of 5.0×10^{-4} per generation (Weber & Wong 1993; Estoup & Angers 1998; Schlötterer 2001; Whittaker *et al.* 2003; Bonhomme *et al.* 2008), which means 1.0×10^{-4} per loci per year corresponding to the sexual maturity age of 5 years for *R. bieti* (Quan & Xie 2002). Prior distributions were uniform and their bounds were set to [0–40] for θ_1, θ_2, and θ_A and [0–5] for m_1 and m_2. For the parameter t, we allowed a wide range of values [0–20]. We ran a number of linked simulations with varying levels of heating (35–80 chains, depending on the populations analysed) required to achieve adequate mixing (Hey & Nielsen 2004). Each chain consisted of 20 000 000 steps and the burn-in was 1 000 000 (Table S3). For credibility intervals, we assessed for each parameter the 90% highest posterior density (HPD) interval, which are the boundaries of the shortest span that includes 90% of the probability density of a parameter.

Recent population bottlenecks can produce distinctive genetic signatures in the distributions of allele size, expected heterozygosity and in the genealogy of microsatellite loci (Cornuet & Luikart 1996; Beaumont 1999; Garza & Williamson 2001; Goossens *et al.* 2006). Here, a commonly used heterozygosity test implemented in Bottleneck (Piry *et al.* 1999) was used to detect for the signature of a recent demographic bottleneck assuming infinite allele, stepwise mutation (SMM) and two-phase mutation models with various (70% to 95%) single-step mutations (Di Rienzo *et al.* 1994). In addition, evidence for demographic change was inferred using MSVAR1.3 (Storz & Beaumont 2002), which implements a coalescent simulation-based Bayesian likelihood analysis, assumes a strict SMM, and estimates the posterior probability distribution of population parameters using MCMC simulation, based on the observed distribution of microsatellite alleles and their repeat number. In every simulation, we ran each chain with 100 000 thinned updates and a thinning interval of 10 000 steps, leading to a total number of 1×10^9 updates. Seven independent simulations were run on five subpopulations using both an exponential and a linear model according the parameter sets used in a study on orangutans (*Pongo pygmaeus*) (Goossens *et al.* 2006).

Results

Two blood, two muscle and 203 fecal samples were collected from 11 monkey groups (G1–G15, no samples form G3, G8, G12 and G14) across the current distribution range (Fig. 1a and Table S4). We were able to amplify mtDNA from 163 out of 207 samples. For samples from the same group, different mtDNA sequence (Liu *et al.* 2007) or microsatellite data with a mismatch of at least two alleles were the criterion for individual identification. Only samples with more than six microsatellite loci data were included. Thus reliable unique genotypes were obtained for 135 (66.2%) out of the 207 samples collected. For these 135 individuals, multilocus genotypes were on average 87.3% complete. A total of 75 alleles were detected from 10 microsatellite loci. The number of alleles observed per locus varied from five to 13, with the overall allelic richness across loci being 7.5. With the multiple-tube approach, only 0.71% of the genotypes were unreliable. The 10 microsatellite loci were in Hardy–Weinberg equilibrium across the population, and overall mean H_O and H_E were 0.614 and 0.703 respectively (Table S4). No loci were in LD across our sampled groups.

Population structure

In the 10 independent simulations of the Bayesian clustering method in Structure, average ln $P(D)$ (−3355.4) was maximized at $K = 5$ but did not decrease dramatically when $K > 5$ (Fig. 2a). Calculation of ΔK from the Structure output produced a distinct apex value (423.9) when $K = 5$ (Fig. 2b). Thus $K = 5$ was the most probable number of genetic clusters within the whole data set in *Rhinopithecus bieti*. The five genetic clusters were largely associated with specific isolated landscape patches (Figs 1a and 2c). Individuals from G1, G2 and G4 formed a northwest cluster (NW) and individuals from G5 the northeast cluster (NE). A central region cluster (C) was formed by individuals from G6, G7, G9 and G10. Groups G11 and G13–G15 were located in the southeast and southwest of the habitat and isolated from other groups.

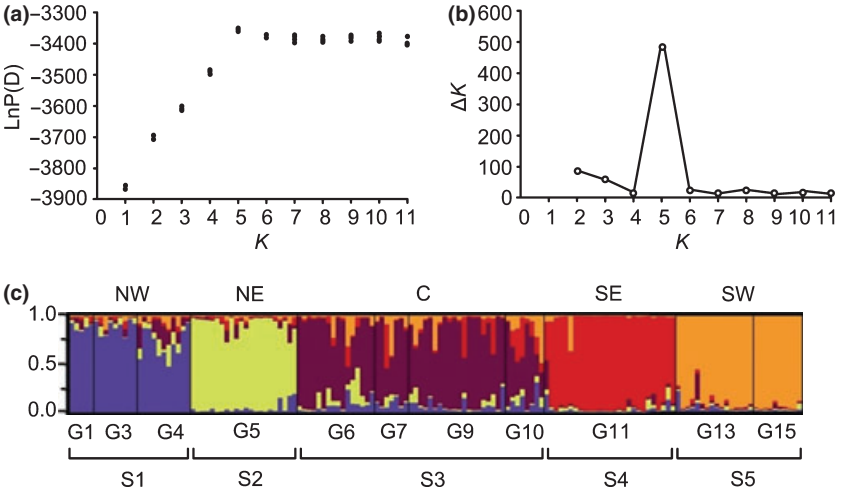

Fig. 2 Structure analysis results. (a) Value of ln $P(D)$ from 10 independent runs for K = 1–11. (b) Value of ΔK as a function of K based on 10 runs. (c) Distribution of the five genetic clusters generated by Structure. The vertical lines are broken into coloured segments showing the proportion of each individual assigned to each of the inferred K. The five genetic clusters are presented by different coloured columns: NW cluster—blue, NE cluster—yellow, C cluster—purple, SE cluster—red, SW cluster—orange. Letters at the bottom of the figure correspond to codes for the sampled groups.

The genetic background of G11 and G13–15 were also revealed to be different and formed the southeast cluster (SE) and southwest cluster (SW) respectively (Fig. 2c). Overall, Structure results indicate that the entire *R. bieti* population is separated into five subpopulations (S1–S5) with a strong spatial pattern (Fig. 2).

Landscape and genetic relationships

When the geo-referenced multilocus genotypes were analysed using software GENELAND, we found the most probable support for five Bayesian population clusters (53% of estimated K-values from GENELAND) (Fig. 3a). Additionally, GENELAND also revealed that '[G1-G4][G5][G6-G10][G11][G13–G15]'were the most probable subdivisions of the entire *R. bieti* population, which verified the population structure inferred by Structure. Each of the identified clusters was spatially contiguous and areas of steep turnover in posterior probabilities of population membership were presumed to reflect barriers to gene flow (Fig. 3b). The spatial pattern of all landscape features is shown in Fig. 1b. Geographic information system (GIS) technology revealed that areas of high quality snub-nosed monkey habitat (coniferous forests and mixed coniferous/broadleaf forests) were interspersed in varying configurations with human-made nonhabitat (farmland, grazing land, main roads, alleys and human resident sites) (Fig. 1b). Comparing Fig. 3b with Fig. 1b, it is clear that gene-flow barriers revealed by GENELAND coincided with spatial distribution of anthropogenic habitat gaps.

Analysis of isolation by distance and isolation by barrier

Genetic distances among monkey groups were measured as pairwise $F_{ST}/(1 - F_{ST})$ and the geographical distances were calculated through GIS analysis

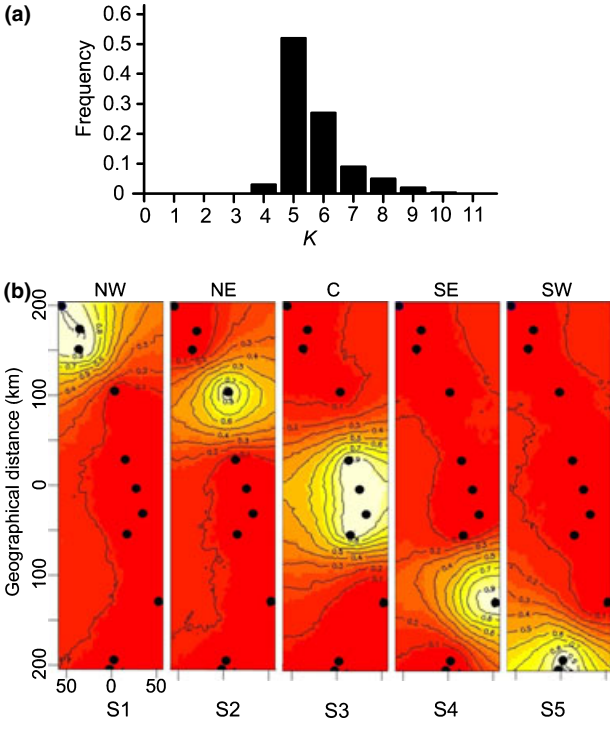

Fig. 3 Bayesian cluster analysis output from GENELAND. (a) The main histogram shows the frequency of inferred K-value across runs. (b) Maps of posterior probabilities to belong to one of K = 5 clusters (NW, NE, C, SW and SE) for 135 individuals of *Rhinopithecus bieti*. Black site indicates core home-range of each sampled group.

(Table 1). Pairwise $F_{ST}/(1 - F_{ST})$ ranged from 0 to 0.2725 and geographical distances spanned from 18.1 to 358.9 km. A categorical matrix was also generated to describe whether the sampled groups are connected by habitat or separated by habitat gaps (Table 1). Isolation-by-distance analysis performed using the Mantel test revealed that 22.09% genetic distance among sampled groups was explained by geographical distance when

Table 1 (a) Genetic and geographical distances between 11 Yunnan snub-nosed monkey groups sampled. Genetic distance is represented by pairwise $F_{ST}/(1 - F_{ST})$ (lower diagonal) and Euclidean geographical distance in km (upper diagonal). (b) Categorical distance matrix describing the presence or absence of habitat gaps among sampled groups

Group	G1	G3	G4	G5	G6	G7	G9	G10	G11	G13	G15
(a) Genetic and geographical distances											
G1		18.1	58.0	110.4	169.7	206.9	210.2	224.0	299.2	345.5	358.9
G3	0.0019		42.0	93.8	153.3	191.8	194.2	209.0	284.6	330.8	344.5
G4	0	0		54.6	111.6	148.8	153.3	167.4	242.8	299.3	301.4
G5	0.1764	0.1493	0.1353		63.3	103.2	102.6	121.6	192.0	242.8	257.7
G6	0.1062	0.1157	0.0583	0.0805		40.6	42.7	58.7	131.0	180.7	195.2
G7	0.1500	0.0923	0.0683	0.1338	0.0410		24.6	18.8	95.5	140.5	155.8
G9	0.0755	0.1110	0.0501	0.1219	0.0226	0.0423		30.9	90.2	143.9	159.6
G10	0.1527	0.1505	0.1113	0.0949	0.0381	0.0749	0.0562		77.6	122.7	136.1
G11	0.2059	0.2525	0.2010	0.1251	0.1231	0.1922	0.1069	0.0627		59.5	77.4
G13	0.0952	0.0799	0.0836	0.1900	0.0864	0.0744	0.0847	0.1315	0.2347		18.9
G15	0.1709	0.1511	0.1562	0.2210	0.1361	0.1193	0.1169	0.1685	0.2725	0.0139	
(b) Categorical distance matrix											
G1											
G3	0										
G4	0	0									
G5	1	1	1								
G6	1	1	1	1							
G7	1	1	1	1	0						
G9	1	1	1	1	0	0					
G10	1	1	1	1	0	0	0				
G11	1	1	1	1	1	1	1	1			
G13	1	1	1	1	1	1	1	1	1		
G15	1	1	1	1	1	1	1	1	1	0	

For sampled monkey groups in contact, the categorical distance between them was 0. In cases where they were isolated by habitat gaps, the categorical distance between them was 1.

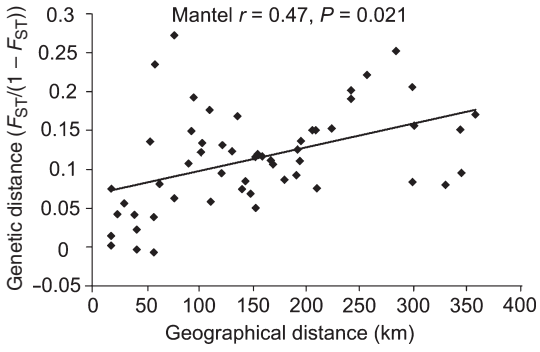

Fig. 4 Isolation-by-distance analysis. There was a positive correlation between geographical distance (km) and genetic distance ($F_{ST}/1 - F_{ST}$) between all pairs of sampling sites. Euclidean geographical distance explains 22.09% of genetic variation in the study area ($r = 0.47$, $P = 0.021$).

the whole study area was considered ($r = 0.47$, $P = 0.021$) (Fig. 4). The Mantel test for the effect of habitat gap on genetic distance confirmed a strong barrier on gene flow and explained 59.29% of genetic differentiation among sampled groups ($r = 0.77$, $P = 0.005$). We also analysed the relationship between geographical distance and the presence of habitat gap, and found that they were highly correlated ($r = 0.59$, $P = 0.000$). The partial Mantel test showed a significant positive correlation between genetic distance and the presence of habitat gaps ($r = 0.51$, $P = 0.01$) after controlling for the effect of geographical distance, and 36.23% of the genetic distance was explained by presence of habitat gaps. Only 4.92% of the genetic distance was explained by geographical distance in partial Mantel test, and no significant correlation between them was found ($r = 0.11$, $P = 0.23$) after controlling for the effect of habitat gaps. The overall variation in genetic distance explained by the model was 41.16%.

Genetic differentiation and migration rate

Genetic differentiation (F_{ST}) among S1–S5 was significant and ranged from 0.1104 to 0.6597 (Table 2) and suggests little migration. Migration rate analysis also indicated that the migration rate between each subpopulation was low, ranging from 0.0028 to 0.0092 (Table 3). Using both previously determined five genetic clusters and geographical sampling locality as prior population information, Structure did not identify any migrants among five subpopulations. GENECLASS 2.0

Table 2 *F*-statistic (F_{ST}) tests for pairwise subpopulation differentiation based on microsatellite loci frequencies

	S1	S2	S3	S4	S5
S1					
S2	0.2213*				
S3	0.1283**	0.1634**			
S4	0.6597**	0.6411**	0.4906**		
S5	0.4448**	0.4439**	0.1104**	0.5663**	

*$P < 0.05$, **$P < 0.01$.

initially identified individual No. 45 from S2 and No. 90 from S4 as first generation migrants (Table 4). However, while both of them have a significant L_h/L_{max} ratio and individual No. 45 has significant L_h, the probability values are very low (0.07 for No. 45, $P < 0.01$; 0.01 for No. 90, $P < 0.01$; Table 4).

Structure also identified a number of individuals not readily classified as first generation migrants, but not clearly assigned as residents either, suggesting that these individuals were the products of admixture between localities. In Structure, potentially admixed individuals are those that do not assign with the majority of individuals from their locality, or which have values of *Q* that indicated nontrivial membership in more than one cluster. Ranking and plotting individual *Q*-values following the approach of Beaumont *et al.* (2001) allowed delineation of a set of samples that did not clearly group into any one cluster (Fig. 5). Based on Structure analysis without prior population information, clear breaks of individual mean *Q*-values are present at $Q = 0.8$ and $Q = 0.2$ (Fig. 5). We defined individuals with mean *Q*-values from 0.8 to 0.2 as potentially admixed (Lecis *et al.* 2006; Vähä & Primmer 2006; Bergl & Vigilant 2007), and individuals with mean *Q*-scores falling exclusively above and below these values assign strongly to one cluster. A total of 114 out of 135 individuals with mean *Q*-values falling exclusively above 0.8 or below 0.2 were assigned to one cluster, while 21 individuals with mean *Q*-values between 0.8 and 0.2 were determined to be composed by at least two clusters. Individual assignments test performed using GENECLASS 2.0 assigned individual No. 45 and No. 90 and other 19 individuals as admixed individuals, which agreed with the Structure results (Table 4). Therefore, no first generation migrant was found in any subpopulation. In addition, 95% posterior probability intervals of *Q* for each individual are shown in Fig. S1.

Population splitting time and population demography

Repeated runs of the IM program revealed unambiguous marginal posterior probability distribution of the parameters for three subpopulation comparisons (S1–S3, S3–S5 and S4–S5; Table 5 and Fig. 6). The peaks of the primary six parameter values were confined to fairly narrow ranges with corresponding credibility intervals illustrated in Fig. 6. The initial splitting time between S1 and S3 was estimated to be 8210 years ago (90% HPD, 5470–13 630). The range of divergence time between S4 and S5 were estimated to be 950 years ago (90% HPD, 510–1640) and implies a recent divergence event. In contrast to the splitting time of above two subpopulation pairs, the initial divergence event between S3 and S5 was estimated to have started 21 550 years ago (90% HPD, 11 960–32 710), which is much earlier than that of S1–S3 and S4–S5. For the population demography estimation, both Bottleneck and MVSAR analysis did not provide convincing evidence for a recent population decline.

Discussion

Population structure and influencing factors

Our results show that the wild population of Yunnan snub-nosed monkeys comprises five subpopulations (S1–S5). For example, monkey groups G1, G2, G3 and G4 in the northwest of the range of this species are connected via narrow forest patches. These four groups share the same genetic background and form subpopulation S1. Northeast subpopulation S2 contains group G5. It is separated from S1 by a band of human resident sites and confined within an isolated small forest surrounded by agricultural area. National Highway 214 forms a major habitat gap separating S1 and S2 from

Table 3 Migration rates between subpopulations (S1–S5) based on microsatellite loci data

	S1	S2	S3	S4	S5
From S1 to		0.00449 (±0.00708)	0.00351 (±0.00543)	0.00329 (±0.00568)	0.00397 (±0.00686)
From S2 to	0.00517 (±0.00847)		0.00278 (±0.00437)	0.00317 (±0.00523)	0.00426 (±0.00707)
From S3 to	0.00918 (±0.01563)	0.007410 (±0.01273)		0.00310 (±0.00552)	0.00521 (±0.00881)
From S4 to	0.00476 (±0.00798)	0.00699 (±0.01266)	0.00665 (±0.01037)		0.00408 (±0.01609)
From S5 to	0.00444 (±0.00750)	0.00445 (±0.00748)	0.00370 (±0.00609)	0.00360 (±0.00519)	

Table 4 Results of first generation migrants and admixed individuals detection analysis

Sample	Geographical origin	Structure (five clusters, no prior population information)	GENECLASS locality	GENECLASS highest assignment probability	GENECLASS F_0 migrant probability (L_h; L_h/L_{max} indicated with ^, *$P < 0.01$)	Structure migrant probability	Final migrant/ admixture classification
No.15	S1-G4	0.447/0.121/0.306/0.036/0.090	S1/S3	0.863/0.966	NS	0.023	AD
No.19	S1-G4	0.659/0.112/0.184/0.029/0.016	S1/S3	0.908/0.708	NS	0.268	AD
No.20	S1-G4	0.631/0.023/0.244/0.039/0.063	S1/S3	0.968/0.998	NS	0.054	AD
No.21	S1-G4	0.508/0.136/0.196/0.029/0.132	S1/S3	0.682/0.828	NS	0.123	AD
No.23	S1-G4	0.588/0.089/0.099/0.065/0.158	S1/S3	0.782/0.717	NS	0.073	AD
No.43	S2-G5	0.044/0.524/0.021/0.385/0.026	S2/S4	0.979/0.560	NS	0.117	AD
No.45	S2-G5	0.195/0.503/0.213/0.014/0.074	S2/S3	0.884/0.943	0.07*	0.155	AD
No.57	S3-G6	0.022/0.382/0.219/0.021/0.356	S2/S3	0.867/0.329	NS	0.042	AD
No.58	S3-G6	0.027/0.451/0.390/0.108/0.023	S2/S3	0.679/0.982	NS	0.090	AD
No.64	S3-G7	0.105/0.051/0.379/0.016/0.449	S3/S5	0.789/0.992	NS	0.140	AD
No.68	S3-G9	0.073/0.164/0.456/0.029/0.278	S2/S3	0.458/0.999	NS	0.100	AD
No.77	S3-G9	0.146/0.084/0.291/0.461/0.018	S3/S4	0.392/0.956	NS	0.127	AD
No.81	S3-G9	0.047/0.091/0.557/0.259/0.047	S3/S4	0.999/0.497	NS	0.051	AD
No.83	S3-G9	0.034/0.176/0.290/0.473/0.028	S2/S3	0.528/0.992	NS	0.087	AD
No.85	S3-G10	0.229/0.067/0.638/0.036/0.030	S1/S3	0.316/0.970	NS	0.069	AD
No.87	S3-G10	0.098/0.063/0.423/0.224/0.191	S3/S4	0.918/0.124	NS	0.076	AD
No.89	S3-G10	0.043/0.014/0.614/0.247/0.082	S3/S4	0.974/0.217	NS	0.055	AD
No.90	S4-G11	0.173/0.061/0.237/0.461/0.067	S3/S4	0.104/0.088	0.01^*	0.256	AD
No.95	S4-G11	0.030/0.036/0.017/0.663/0.254	S4/S5	0.881/0.792	NS	0.109	AD
No.103	S4-G11	0.009/0.059/0.096/0.814/0.022	S3/S4	0.840/0.846	NS	0.038	AD
No.116	S5-G12	0.044/0.032/0.191/0.039/0.694	S3/S5	0.858/0.922	NS	0.097	AD

AD, admixed individual.

^ means the P value of $L_h < 0.01$, * means the P value of $L_h/L_{max} < 0.01$.

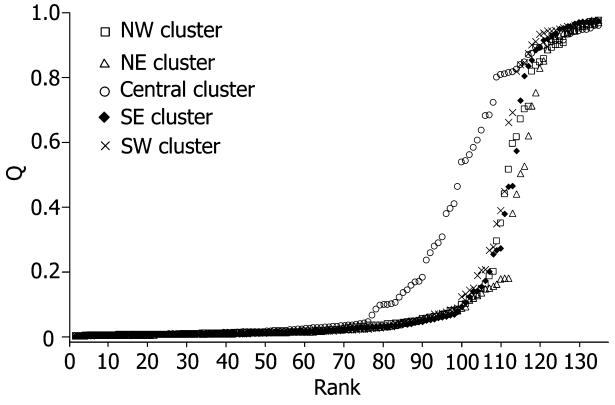

Fig. 5 Ranked mean Q (proportional membership in each cluster) for each individual in each cluster. Admixed individuals have values between 0.2 and 0.8.

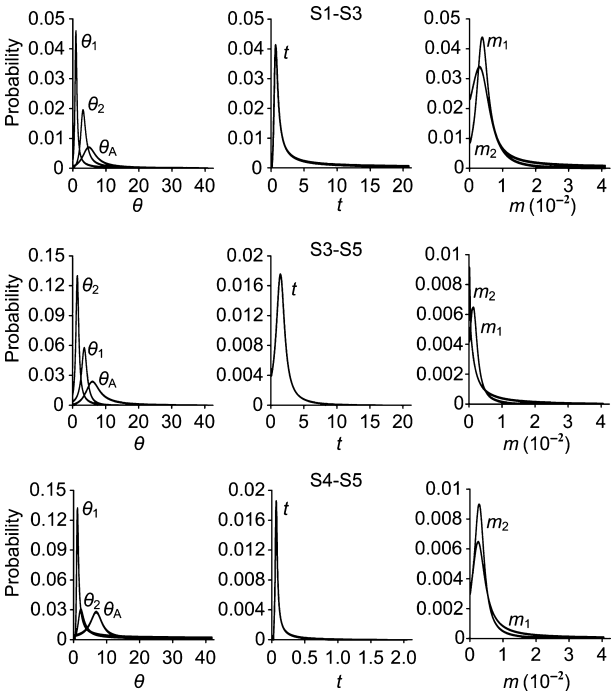

Fig. 6 Multilocus posterior distributions of demographic parameters estimated with the IM program, using 10 microsatellite loci. The effective population sizes, migration rates, and divergence time are scaled by the neutral mutation rate (corresponding to θ_1, θ_2, θ_A, m_1, m_2, t).

the central subpopulation S3. The central region is large and well preserved compared with other patches and *Rhinopithecus bieti* groups (G6–G10) of the central subpopulation (S3) are connected via forest corridors. For the southeast subpopulation S4 and southwest S5, they are completely surrounded by dense arable land, road networks and human dwellings. These southern subpopulations (S4 and S5) are isolated both from each other and other subpopulations.

Fine-scale population structure is common in large mammals and can been influenced by various internal and external factors (Macey *et al.* 1998; Hendry *et al.* 2008; Jin *et al.* 2008). Among internal causes, social structure is a key issue which is largely mediated by social behaviour (reproductive skew, dispersal, group fission and fusion patterns) (Lampert *et al.* 2003; Modolo *et al.* 2008). In the *Rhinopithecus* genus, wild groups are typically based on small family units of five to15 individuals composed of a single male and multiple females and their offspring (referred to as a one male unit or OMU). OMUs range together as larger groups of 50 to over 200 animals. All male units (AMUs) composed of two to five adults or subadult males are also common (Kirkpatrick 1998; Long *et al.* 1994). Female individuals usually remain in the natal group and AMUs leave the natal group during breeding season to find mating opportunities in neighbouring groups (Kirkpatrick 1998; Ren 1999). Female philopatry is known to result in significant genetic differentiation in maternally inherited genetic markers. Previous studies have shown that the distribution of mtDNA haplotypes of *R. bieti* display strong geographical specificity;

Table 5 Maximum-likelihood estimates (MLEs) and 90% HPD intervals of demographic parameters of the IM model

Comparison	θ_1	θ_2	θ_A	m_1	m_2	t	T (years)
S1–S3							
MLE	1.1153	3.4639	5.8402	0.0056	0.0046	0.8210	8210
Lower 90% HPD	0.3613	1.9579	1.1881	0.0027	0.0011	0.5470	5470
Upper 90% HPD	2.1521	5.1039	12.232	0.0072	0.0065	1.3630	13 630
S3–S5							
MLE	1.8550	3.5644	7.0503	0.0025	0.0008	2.1550	21 550
Lower 90% HPD	0.6554	1.6901	2.2442	0.0009	0.0003	1.1960	11 960
Upper 90% HPD	2.6016	5.4386	14.755	0.0041	0.0023	3.2710	32 710
S4–S5							
MLE	2.7519	1.2497	6.5117	0.0041	0.0067	0.0950	950
Lower 90% HPD	0.7842	0.5481	2.9599	0.0025	0.0033	0.0510	510
Upper 90% HPD	5.6607	2.2144	10.063	0.0089	0.0081	0.1640	1640

however, common haplotypes are still shared between subpopulations (Liu *et al.* 2007).

Here, social structure could have contributed to genetic differentiation between subpopulations of *R. bieti*, but it might not to be the pivotal cause that explains the fine-scale population structure revealed by microsatellite loci. In cercopithecines, males typically immigrate to neighbouring social groups, providing substantial levels of gene flow per generation that counteract genetic differentiation at autosomal loci (Pusey & Packer 1987; Oi 1988; Di Fiore 2003). Predictions of genetic consequences due to male-biased dispersal in cercopithecines would be different between autosomal and maternally inherited genetic markers. Previous studies based on autosomal loci revealed genetic homogenization and very limited genetic differentiation between social groups in natural populations of long-tailed macaques (*Macaca fascicularis*) and Barbary macaques (*Macaca sylvanus*) (Kawamoto *et al.* 1982; de Ruiter 1994; de Ruiter & Geffen 1998; von Segesser *et al.* 1999). In our study, the most notable feature of *R. bieti* population structure is the genetic discontinuity between subpopulations and the coincidence with the anthropogenic landscape features. Although gene flow revealed by microsatellite loci is also low between subpopulations, it is assumed to be the result of disruption to male-based dispersal rather than female philopatry. Notably, G13 and G15 in S5 also share no common mtDNA haplotype (H23–H28 existed in G13 and H29–H30 existed in G15) (Liu *et al.* 2007); however, gene flow between G13 and G15 appears sufficient as these two social groups show homogenization in genetic background (Fig. 2).

Habitat discontinuity between subpopulations may play a key role in shaping *R. bieti* population structure. Areas of genetic discontinuity revealed by GENELAND are consistent with the spatial distribution of anthropogenic landscape features. Satellite imaging and GIS analysis revealed that areas of high quality Yunnan snub-nosed monkey habitat (coniferous forests and mixed coniferous/broadleaf forests) are interspersed in varying configurations with anthropogenic nonhabitat (arable land, grazing meadow, main roads, alleys and human resident sites) (Fig. 1b). Subpopulations of *R. bieti* are limited in insular forest patches, which are surrounded by arable land, roads and human habitation. In S1, S3 and S5, monkey groups are still connected via forest corridors which permit mating opportunities between groups. This could explain the genetic proximity of monkey groups within the same subpopulation. However, dispersal hardly occurred in areas where human activity is highly concentrated despite that *R. bieti* have been observed spending time on the ground and to travel between forest patches (Mu & Yang 1984; Bai *et al.* 1987; Wu *et al.* 1988; Wu 1993; Kirkpatrick & Long 1994; Kirkpatrick 1996). In summary, gene flow between subpopulations revealed by nuclear microsatellite loci was low, yet gene flow between groups within subpopulations was well preserved.

Effect of landscape features on R. bieti *across time*

Our estimation of when the population underwent structuring revealed factors that have influenced present-day population structure. The time at which subpopulations began diverging was found to have occurred between 21 550 and 950 years ago and suggests that both biogeographical and anthropogenic landscape features played a role. *Rhinopithecus bieti* is found only in coniferous and mixed coniferous/broadleaf forests along ridge-top 'islands' of the Yunling Mountain (Jablonski 1993; Long *et al.* 1994). The time of initial divergence between S3–S5 is *c.* 21 550 years ago (90% HPD, 11 960–32 710) and coincides with the last glacial maximum (17 000–23 000 years ago). During the last glacial maximum, ice sheets filled valleys and covered lowlands and high montane forests might have acted as refuges for *R. bieti* (Shi *et al.* 1998; Jablonski 1993; Zhang *et al.* 2002).

Although the climate became warmer and drier following the last glacial maximum and forest zones may have reconnected on one occasion, vegetation variation and human colonization since the Holocene further isolated *R. bieti* groups (Walker 1986; Shi *et al.* 1998; Zhang *et al.* 2002). During climatically induced faunal displacement, disjunctions frequently developed in cold-adapting boreal-alpine species of the Holarctica (Illies 1974). Warm weather and vegetation variation during the Holocene might also constrict conifer forests to mountain-tops (Jablonski 1993; Kirkpatrick 1995). Most importantly, archeological records indicate an increase in human exploitation of the Tibetan Plateau commencing 10 000 years ago (Lu & Teng 2006). Several prehistoric anthropogenic relics dated at 5500–4300 years old have been located in present *R. bieti* habitat. In addition, National Highway 214 was a historically famous commercial road named 'The ancient tea-horse road' and has played a crucial role in cultural exchange between Han and Tibetan people (Chen 2006; Nangsa 2007; Zi 2007). Although the modern highway has been present for only several decades, human activity along this ancient route can be traced back to the late Neolithic age (5000–4000 years ago) and even earlier according to Tibetan language records and archaeological findings (Shi 2003; Zhang 2005). Evidence of large-scale human exploitation in this region can be dated to 3000 years ago using a small number of ancient texts, yet earlier detailed data were limited (Ho 1959; Cao 2001). Records of recent agricultural history within the last 500 years

Table 6 Evolutionary model of population structure in *Rhinopithecus bieti*. Results of multiple analyses and supporting references are listed

Time (years ago)	Results and references	Inference	Analysis	Software
21 550 (11 960–32 710)	1. Initial divergence between S3 & S5 2. Glacial vestiges in habitat of *R. bieti*	Population divergence caused by the last glacial maximum (17 000–23 000 years ago)	Analysis of population structure evolution	IM
8210 (5470–13 630)	1. Initial divergence between S1 & S3 2. Prehistoric anthropogenic relics 3. Tibetan language records and archaeological materials	Population divergence caused by human activity since Holocene		
950 (510–1640)	1. Initial divergence between S4 & S5 2. Large scale human exploitation since 3000 years ago 3. 10-fold increase of arable area and 17.7-fold increase of human population during the past 500 years	Population divergence caused by large scale human exploitation during the past thousand years		
At present	1. Five subpopulations 2. Significant genetic differentiation	Significant population structure	Population structure analysis	1. Structure 2. GENELAND
	1. Genetic discontinuity was consistent with the spatial distribution of anthropogenic landscape features 2. Significant positive correlation between genetic distance and the presence of habitat gaps	Anthropogenic genetic discontinuity	1. Landscape analysis using satellite imagery 2. Landscape genetics analysis 3. IBD and IBB analysis	1. ARCGIS 2. GENELAND 3. Mantel test 4. Partial Mantel test
	1. Low migration rate 2. No first generation migrant was found	Obstructed gene flow from anthropogenic habitat gaps	1. Migration rate test 2. Detection of migrant and admixed individuals	1. BAYESASS 2. GENECLASS 3. Structure

are more abundant. According to historical county annals, over the last 500 years this region has experienced a 10-fold increase (25 670–262 601 km^2) of arable land and a 17.7-fold human population increase ($R^2 = 0.962$, $P = 0.001$) [ancient reference: *Yunnan Annal of Emperor Zhengde, Ming Dynasty* (1510), *Yunnan Record of Qing Dynasty* (1731), *Yunnan Record of Qing Dynasty* (1811, 1830), *Yunnan Annal of Emperor Jia Qing, Qing Dynasty* (1884), *The National Population Census of People's Republic of China* (1952, 1982, 2000)]. Furthermore, the southern boundary of *R. bieti* habitat has shifted 100 km northward during the past 400 years as a result of rapidly expanding levels of human exploitation (Li *et al.* 2002). The initial splitting time of S1–S3 and S4–S5 was estimated to be 8210 years ago (90% HPD, 5470–13 630 years ago) and 950 years ago (90% HPD, 510–1640 years ago), respectively, and this is consistent with the time of initial human encroachment and later large scale human exploitation.

Our analyses aimed to detect the present population structure and determine causal factors that may have impacted upon this species, From the IM analysis, it is inferred that both historical environmental changes and human-induced effects, or a combination of both, have shaped the evolutionary process of *R. bieti* population genetic structuring. Landscape genetic, tion by distance (IBD)/isolation by barrier (IBB) and migration analysis indicated that the anthropogenic barriers between subpopulations have played a key role in shaping the present-day *R. bieti* population structure. When interpreting

our results, we have drawn on climatic and anthropogenic patterns and propose a consistent evolutionary model for population structuring in this animal (Table 6): initial divergence caused by the Last Glacial Maximum followed by a warm Holocene and changes in vegetation allowed continued human encroachment into flat valleys and resulted in further isolation of *R. bieti* subpopulations and enhanced genetic differentiation.

Conservation implication

According to the model proposed by Moritz (1994), the five subpopulations (S1–S5) of *R. bieti* should be considered as five management units and forest corridors between subpopulations should be re-established. However, the matrix between subpopulations is composed of national highways, agricultural fields, towns and villages and vegetation restoration is impractical because of the high expense of relocating highways and human dwellings. Therefore, the first step should be to prevent further fragmentation between groups still in migratory contact within subpopulations. For example, four groups (G1–G4) in subpopulation S1 are still connected via narrow forest corridors and some effort should be made to enhance this forest (Fig. 1). Other sections of *R. bieti* habitat were exposed to fragmentation in varying degrees. In subpopulation 5, G15 has been already separated from G13 and G14 through agricultural activity. Although the degree and duration of fragmentation are probably not yet enough to create genetic differentiation within subpopulations, such isolation is likely if current conditions continue. Therefore, the ongoing habitat degeneration should be halted. We have defined five priority restoration regions (pr1–pr5) that represent pivotal areas for migration within subpopulations (Fig. 1a). Other potential solutions, such as periodic individual/family unit translocation, should be discussed with comprehensive conservation knowledge of this species through long-term conservation practice.

Conclusion

Although anthropogenic influences on population genetics and historical demographic changes of wild animals have been found around the world (Goossens *et al*. 2006; Hendry *et al*.2008; Smith *et al*.2008; Waples *et al*. 2008), we are unaware of any study emphasizing the impact of human-made landscapes on the genetic structure of wild animals inhabiting the Tibetan Plateau. Even in what is considered a remote and relatively intact environment, gene flow between subpopulations of *Rhinopithecus bieti* appears to be strongly impeded by arable land, grazing meadows, highways and humans dwellings. Although genetic differentiation between *R. bieti* subpopulations could be explained by other factors (climate change, social structure and habitat landform), our findings show that increasing human influence resulting in habitat fragmentation is an important factor in shaping the genetic structure and evolutionary potential of *R. bieti*. Therefore, conservation strategies are needed to reduce the impact of human activity on wildlife habitat that prevent further fragmentation. We hope our research provides a model for similarly distributed organisms on the Tibetan Plateau also affected by human activity.

Acknowledgements

This project was supported by the National Basic Research Program of China (973 Program: 2007CB411600), Natural Science Foundation of China (No. 30630016 and No.30570292), Innovation Project of the Chinese Academy of Sciences (KSCX2-YW-R-091), Nature Conservancy (TNC) and State Forestry Administration of China. Thanks to Michael Bruford (Cardiff University, UK), Linda Vigilant (Max Planck Institute for Evolutionary Anthropology, Germany) and Yi Tao for technical guidance and data analysis and to Geoffrey Hobbs, Ben Bravery, Mary Blair, Z.L. Wang, X.J. Zhan, D.W. Qi and M. Lu for their laboratory assistance and suggestions.

References

Bai SC, Zou SQ, Lin S *et al*. (1987) A preliminary observation on distribution, number and population structure of *Rhinopithecus bieti* in Baima Xueshan Nature Reserve, Yunnan, China. *Zoology Research*, **8**, 413–419.

Beaumont MA (1999) Detecting population expansion and decline using microsatellites. *Genetics*, **153**, 2013–2029.

Beaumont M, Barratt EM, Gottelli D *et al*. (2001) Genetic diversity and introgression in the Scottish wildcat. *Molecular Ecology*, **10**, 319–336.

Belkhir K (2004) GENETX, *Logiciel sous Windows TM pour la Génétique des Populations*. Université de Montpellier II, Montpellier.

Bergl AR, Vigilant L (2007) Genetic analysis reveals population structure and recent migration within the highly fragmented range of the Cross River gorilla (*Gorilla gorilla diehli*). *Molecular Ecology*, **16**, 63–72.

Bonhomme M, Blancher A, Cuartero S *et al*. (2008) Origin and number of founders in an introduced insular primate: estimation from nuclear genetic data. *Molecular Ecology*, **17**, 1009–1019.

Brumfiel G (2008) Acclaimed photo was faked. *Nature*, **451**, 1034–1035.

Cao SJ (2001) *The History of Chinese Population*. Publishing House of Fudan University, Shanghai.

Chen T (2006) Yadong skirted by the Tea-Horse Trade Route. *China's Tibet*, **17**, 4–11.

Cincotta RP, Wisnewski J, Engelman R (2000) Human population in the biodiversity hotspots. *Nature*, **404**, 990–992.

Cornuet JM, Luikart G (1996) Description and power analysis of two tests for detecting recent population bottlenecks from allele frequency data. *Genetics*, **144**, 2001–2014.

Cornuet JM, Piry S, Luikart G *et al.* (1999) New methods employing multilocus genotypes to select or exclude populations as origins of individuals. *Genetics*, **153**, 1989–2000.

Creel S, Spong G, Sands JL *et al.* (2003) Population size estimation in Yellowstone wolves with error-prone non-invasive microsatellite genotypes. *Molecular Ecology*, **12**, 2003–2009.

Di Fiore A (2003) Molecular genetic approaches to the study of primate behavior, social organization, and reproduction. *Yearbook of Physical Anthropology*, **46**, 62–99.

Di Rienzo A, Peterson AC, Garza JC *et al.* (1994) Mutational processes of simple-sequence repeat loci in human populations. *Proceedings of the National Academy of Sciences, USA*, **91**, 3166–3170.

Estoup A, Angers B (1998) Microsatellites and minisatellites for molecular ecology: theoretical and empirical considerations. In: *Advances in Molecular Ecology* (ed. Carvalho G), pp. 55–86. NATO ASI Series, IOS Press, Amsterdam.

Evanno G, Regnaut S, Goudet J (2005) Detecting the number of clusters of individuals using the software structure: a simulation study. *Molecular Ecology*, **14**, 2611–2620.

Excoffier L, Laval G, Schneider S (2005) ARLEQUIN (version. 3.0): an integrated software package for population genetics data analysis. *Evolutionary Bioinformatics Online*, **1**, 47–50.

Garza JC, Williamson EG (2001) Detection of reduction in population size using data from microsatellite loci. *Molecular Ecology*, **10**, 305–318.

Goossens B, Chikhi L, Ancrenaz M *et al.* (2006) Genetic signature of anthropogenic population collapse in Orang-utans. *PLoS Biology*, **4**, 0285–0291.

Goudet J (2002) *FASTA: A program to estimate and test gene diversities and fixation indices*. Institute of Ecology, Lausanne.

Guillot G, Mortier F, Estoup A (2005) GENELAND: a computer package for landscape genetics. *Molecular Ecology Notes*, **5**, 712–715.

Guo SW, Thompson EA (1992) Performing the exact test of Hardy–Weinberg proportion for multiple alleles. *Biometrics*, **48**, 359.

Hanski IA, Gilpin M (1997) *Metapopulation Biology: Ecology and Evolution*. Academic Press, Toronto.

Hao YL, Liu ZJ, Wu H *et al.* (2007) Isolation and characterization of 11 microsatellite loci for the Sichuan snub-nosed monkey, *Rhinopithecus roxellana*. *Conservation Genetics*, **8**, 1021–1024.

Hayaishi S, Kawamoto Y (2006) Low genetic diversity and biased distribution of mitochondrial DNA haplotypes in the Japanese macaque (*Macaca fuscata yakui*) on Yakushima Island. *Primates*, **47**, 158–164.

Hendry AP, Farrugia TJ, Kinneson MT (2008) Human influences on rates of phenotypic change in wild animal populations. *Molecular Ecology*, **17**, 20–29.

Hewitt G (2000) The genetic legacy of the Quaternary ice age. *Nature*, **405**, 907–913.

Hey J (2006) Recent advances in assessing gene flow between diverging populations and species. *Current Opinion in Genetics and Development*, **16**, 592–596.

Hey J, Nielsen R (2004) Multilocus methods for estimating population sizes, migration rates and divergence time, with applications to the divergence of *Drosophila pseudoobscura* and *D. persimilis*. *Genetics*, **167**, 747–760.

Ho PT (1959) *Studies on the Population of China 1368–1953*. Harvard University Press, Cambridge, Massachusetts, London.

Ihaka R, Gentleman R (1996) R: a language for data analysis and graphics. *Journal of Computational and Graphical Statistics*, **5**, 299–314.

Illies J (1974) *Introduction to Zoogeography*. The Macmillan Press Ltd, London, 57 pp.

Jablonski NG (1993) Quaternary environments and the evolution of primates in east Asia, with notes on two new specimens of fossil Cercopithecidae from China. *Folia Primatology*, **60**, 118–132.

Jin YT, Brown RP, Liu NF (2008) Cladogenesis and phylogeography of the lizard *Phrynocephalus vlangalii* (Agamidae) on the Tibetan plateau. *Molecular Ecology*, **17**, 1971–1982.

Kawamoto Y, Takenaka O, Brotoisworo E (1982) Preliminary report on genetic variations within and between species of Sulawesi macaques. *Kyoto University Overseas Research Report of Studies of Asian Non-Human Primates*, **2**, 23–37.

Kirkpatrick RC (1995) The natural history and conservation of the snub-nosed monkeys (genus *Rhinopithecus*). *Biological Conservation*, **72**, 363–369.

Kirkpatrick RC (1996) *Ecology of the Yunnan Snub-nosed Langur* Rhinopithecus bieti *(Colobinae) in the Conifer forests of Baimaxueshan Nature Reserve, People's Republic of China*. PhD Dissertation, University of California, Davis.

Kirkpatrick RC (1998) Ecology and Behavior in the Snub-nosed and Douc Langurs. In: *The Natural of the Doucs and Snub-nosed Monkey* (ed. Jablonski NG), pp. 155–190. World Scientific Publishing, Singapore.

Kirkpatrick RC, Long YC (1994) Altitudinal ranging and terrestriality in the Yunnan snub-nosed monkey (*Rhinopithecus bieti*). *Folia Primatology*, **63**, 102–106.

Lampert KP, Rand AS, Mueller UG *et al.* (2003) Fine-scale genetic pattern and evidence for sex-biased dispersal in the túngara frog, *Physalaemus pustulosus*. *Molecular Ecology*, **12**, 3325–3334.

Lande R, Barrowclough G (1987) Effective population size, genetic variation and their use in population management. In: *Viable Populations for Conservation* (ed. Soulé ME), pp. 87–123. Cambridge University Press, New York.

Lecis R, Pierpaoli M, Biro ZS *et al.* (2006) Bayesian analyses of admixture in wild and domestic cats (*Felis silvestris*) using linked microsatellite loci. *Molecular Ecology*, **15**, 119–132.

Li BG, Pan RL, Oxnard CE (2002) Extinction of snub-nosed monkeys in China during the past 400 years. *International Journal of Primatology*, **23**, 1227–1244.

Liu JQ, Wang YJ, Wang AL *et al.* (2006) Radiation and diversification within the Ligularia–Cremanthodium–Parasenecio complex (Asteraceae) triggered by uplift of the Qinghai-Tibetan Plateau. *Molecular Phylogenetics and Evolution*, **38**, 31–49.

Liu ZJ, Ren BP, Wei FW *et al.* (2007) Phylogeography and population structure of Yunnan snub-nosed monkey (*Rhinopithecus bieti*) inferred from mitochondrial control region DNA sequence analysis. *Molecular Ecology*, **16**, 3334–3349.

Liu ZJ, Ren BP, Hao YL *et al.* (2008) Identification of 13 human microsatellite markers cross-species amplification for fecal

samples from Yunnan snub-nosed monkey (*Rhinopithecus bieti*). *International Journal of Primatology*, **29**, 265–272.

Long YC, Kirkpatrick C, Zhong T *et al.* (1994) Report on the distribution, population, and ecology of the Yunnan snub-nosed monkey. *Primates*, **35**, 241–250.

Long YC, Kirkpatrick C, Zhong T *et al.* (1996) Status and conservation strategy of the Yunnan snub-nosed monkey. *Chinese Biodiversity*, **4**, 145–152.

Lu Y, Teng ZZ (2006) *The Study of Historical Province Population Size in China*. Shandong People's Press, Jinan, 535 pp.

Luo J, Yang DM, Suzuki H *et al.* (2004) Molecular phylogeny and biogeography of Oriental voles: genus Eothenomys (Muridae, Mammalia). *Molecular Phylogenetics and Evolution*, **33**, 349–362.

Macey JR, Schulte JA II, Larson A *et al.* (1998) Phylogenetic relationships of toads in the *Bufu bufo* species group from the eastern escarpment of the Tibetan Plateau: a case of vicariance and dispersal. *Molecular Phylogenetics and Evolution*, **9**, 80–87.

Manel S, Schwartz M, Luikart G *et al.* (2003) Landscape genetics: combining landscape ecology and population genetics. *Trends in Ecology and Evolution*, **18**, 189–197.

Mantel N (1967) The detection of disease clustering and a generalized regression approach. *Cancer Research*, **27**, 209–220.

Modolo L, Martin RD, Schaik CPV *et al.* (2008) When dispersal fails: unexpected genetic separation in Gibraltar macaques (*Macaca sylvanus*). *Molecular Ecology*, **17**, 4027–4038.

Moritz C (1994) Applications of mitochondrial DNA analysis in conservation: a critical review. *Molecular Ecology*, **3**, 401–411.

Mu WW, Yang DH (1982) A primary observation on the group figures, moving lines and food of *Rhinopithecus bieti* at the east side of Baima-snow Montain. *Acta Theriology Sina*, **2**, 125–131.

Myers N, Mittermeier RA, Mittermeier CG *et al.* (2000) Biodiversity hotspots for conservation priorities. *Nature*, **403**, 853–858.

Nangsa L (2007) *The Ancient Sichuan-Tibet Tea-Horse Road*. Foreign Language Press, Beijing.

Nielsen R, Wakeley J (2001) Distinguishing migration from isolation: a Markov chain Monte Carlo approach. *Genetics*, **158**, 885–896.

Oi T (1988) Sociological study on the troop fission of wild Japanese monkeys (*Macaca fuscata yakui*) on Yakushima Island. *Primates*, **29**, 1–19.

Paetkau D, Slade R, Burden M *et al.* (2004) Genetic assignment methods for the direct, real-time estimation of migration rate: a simulation-based exploration of accuracy and power. *Molecular Ecology*, **13**, 55–65.

Peng Z, Ho SYW, Zhang Y *et al.* (2006) Uplift of the Tibetan plateau: evidence from divergence times of glyptosternoid catfishes. *Molecular Phylogenetics and Evolution*, **39**, 568–572.

Piry S, Luikart G, Cornuet JM (1999) Bottleneck: a computer program for detecting recent reductions in the effective size using allele frequency data. *Journal of Heredity*, **90**, 502–503.

Piry S, Alapetite A, Cornuet JM *et al.* (2004) GENECLASS 2: a software for genetic assignment and first-generation migrant detection. *Journal of Heredity*, **95**, 536–539.

Pritchard JK, Stephens M, Donnelly PJ (2000) Inference of population structure using multilocus genotype data. *Genetics*, **155**, 945–959.

Pusey AE, Packer C (1987) Dispersal and philopatry. In:*Primate Societies* (eds Smuts BB, Cheney DL, Seyfarth RM, Wrangham RW, Struhsaker TT), pp. 250–266. The University of Chicago Press, Chiago.

Qu YH, Ericson PGP, Lei FM *et al.* (2005) Postglacial colonization of the Tibetan plateau inferred from the matrilineal genetic structure of the endemic red-necked snow finch, *Pyrgilauda ruficollis*. *Molecular Ecology*, **14**, 1767–1781.

Qu Y, Ericson PGP, Lei F *et al.* (2006) Molecular phylogenetic relationship of snow finch complex (genera *Montifringilla*, *Pyrgilauda*, and *Onychostruthus*) from the Tibetan plateau. *Molecular Phylogenetics and Evolution*, **40**, 218–226.

Quan GQ, Xie JY (2002) *Research on the Golden Monkey*. Science and Education Publishing House, Beijing.

Rannala B, Mountain JL (1997) Detecting immigration by using multilocus genotypes. *Proceedings of the National Academy of Sciences, USA*, **94**, 9197–9201.

Raymond M, Rousset F (2003) GENEPOP version 3.4: updated from GENEPOP version 1.2, population genetics software for exact tests and ecumenicism. *Journal of Heredity*, **8**, 248–249.

Ren BP (1999) *Spatial distribution patterns in a group of the Sichuan snub-nosed monkeys (*Rhinopithecus roxellana*) in Qinling Region*. MS thesis, Northwest University, Xi'an (in Chinese).

Rousset F (1997) Genetic differentiation and estimation of gene flow from F-statistics under isolation by distance. *Genetics*, **145**, 1219–1228.

Ruan LZ, Zhang LX, Wen LY *et al.* (2005) Phylogeny and molecular evolution of Tetraogallus in China. *Biochemical Genetics*, **43**, 507–518.

de Ruiter JR (1994) *Behaviour and Genes in Natural Populations of Long-Tailed Macaques (*Macaca fascicularis*)*. University of Utrecht, Utrecht, The Netherlands.

de Ruiter JR, Geffen E (1998) Relatedness of matrilines, dispersing males and social groups in long-tailed macaques (*Macaca fascicularis*). *Proceedings of the Royal Society of London. Seires B: Biological Sciences*, **265**, 79–87.

Ryman N, Jorde PE (2001) Statistical power when testing for genetic differentiation. *Molecular Ecology*, **10**, 2361–2374.

Sambrook J, Fritsch EF, Maniatis T (1989) *Molecular Cloning: A Laboratory Manual*, 2nd edn. Cold Spring Harbor Laboratory Press, New York.

Schlötterer C (2001) Evolutionary dynamics of microsatellite DNA. *Chromosoma*, **109**, 365–371.

von Segesser F, Ménard N, Gaçi B, Martin RD (1999) Genetic differentiation within and between isolated Algerian subpopulations of Barbary macaques (*Macaca sylvanus*): evidence from microsatellites. *Molecular Ecology*, **8**, 433–442.

Shi S (2003) Changdu: junction on the ancient Tea-Horse road and its ancient culture. *Journal of Tibet University*, **18**, 12–20.

Shi YF, Li JJ, Li BY (1998) *Uplift and Environmental Changes of Qinghai-Xizang (Tibetan) Plateau in the Late Cenozoic*. Science and Technology Press, Guangzhou.

Simberloff D (1988) The contribution of population and community biology to conservation science. *Annual Review of Ecology and Systematics*, **19**, 473–511.

Smith TB, Milà B, Grether GF *et al.* (2008) Evolutionary consequences of human disturbance in a rainforest bird species from Central Africa. *Molecular Ecology*, **17**, 58–71.

Smouse PE, Long JC, Sokal RR (1986) Multiple regression and correlation extensions of the Mantel test of matrix correspondence. *Systematic Zoology*, **35**, 627–632.

Storz JF, Beaumont MA (2002) Testing for genetic evidence of population expansion and contraction: an empirical analysis of microsatellite DNA variation using a hierarchical Bayesian model. *Evolution*, **56**, 154–166.

Taberlet P, Luikart G (1999) Non-invasive genetic sampling and individual identification. *Biological Journal of the Linnean Society*, **68**, 41–55.

Taberlet P, Griffin S, Goossens B *et al.* (1996) Reliable genotyping of samples with very low DNA quantities using PCR. *Nucleic Acids Research*, **24**, 3189–3194.

Vähä J, Primmer CR (2006) Efficiency of model-based Bayesian methods for detecting hybrid individuals under different hybridization scenarios and with different numbers of loci. *Molecular Ecology*, **15**, 63–72.

Walker D (1986) Late Pleistocene-early Holocene vegetational and climacitc changes in Yunnan Province, southwest China. *Journal of Biogeography*, **13**, 477–486.

Waples RS, Zabel RW, Scheurell MD *et al.* (2008) Evolutionary responses by native species to major anthropogenic changes to their ecosystems: Pacific salmon in the Columbia River hydropower system. *Molecular Ecology*, **17**, 84–96.

Weber JL, Wong C (1993) Mutation of human short tandem repeats. *Human Molecular Genetics*, **2**, 1123–1128.

Weir BS (1979) Inferences about linkage disequilibrium. *Biometrics*, **35**, 235–254.

Weir BS, Cockerham CC (1984) Estimating F statistics for the analysis of population structure. *Evolution*, **38**, 1358–1370.

Whittaker JC, Harbord RM, Boxall N *et al.* (2003) Likelihood-based estimation of microsatellite mutation rates. *Genetics*, **164**, 781–787.

Wilson GA, Rannala B (2003) Bayesian inference of recent migration rates using multilocus genotypes. *Genetics*, **163**, 1177–1191.

Wright S (1978) *Evolution and the Genetics of Populations*. University of Chicago Press, Chicago.

Wu BQ (1993) Patterns of spatial dispersion, locomotion and foraging behaviour in three groups of the Yunnan snub-nosed langur (*Rhinopithecus bieti*). *Folia Primotology*, **60**, 63–71.

Wu SG, Feng ZJ (1992) The general characteristics, conservation and utilization of biological resources in the Qinghai-Xizang Plateau. In: *Proceedings of the First Symposium on the Qinghai-Xizang Plateau* (eds Tong W, Deng WM, Feng XH *et al.*), pp. 163–169. Science Press, Beijing, China.

Wu BQ, Zhong T, Ji W (1988) A preliminary survey of ecology and behavior on a Yunnan snub-nosed monkey (*Rhinopithecus bieti*) group. *Zoology Research*, **9**, 371–384.

Xiao W, Ding W, Cui LW *et al.* (2003) Habitat Degradation of *Rhinopithecus bieti* in Yunnan, China. *International Journal of Primatology*, **24**, 389–398.

Yang DH (1984) Locomotor characters of *Rhinopithecus bieti*. *Acta Theriology Sina*, **4**, 34, 62.

Yang Q, Xia L (2008) Tibetan wildlife is getting used to the railway. *Nature*, **452**, 810–811.

Yu FH, Yu FR, McGuire PM *et al.* (2004) Molecular phylogeny and biogeography of woolly flying squirrel (Rodentia: Sciuridae), inferred from mitochondrial cytochrome b gene sequences. *Molecular Phylogenetics and Evolution*, **33**, 735–744.

Zhan XJ, Li M, Zhang Z *et al.* (2006) Molecular censusing doubles giant panda population estimate in a key nature reserve. *Current Biology*, **16**, 451–452.

Zhang Y (2005) Tea-Horse trade route linking Tibet with the Hinterland. *China's Tibet*, **16**, 46–49.

Zhang FF, Jiang ZZ (2006) Mitochondrial phylogeography and genetic diversity of Tibetan gazelle (*Procapra picticaudata*): implications for conservation. *Molecular Phylogenetics and Evolution*, **41**, 313–321.

Zhang BP, Chen XD, Li BL *et al.* (2002) Biodiversity and conservation in the Tibetan Plateau. *Journal of Geographical Science*, **12**, 135–143.

Zi Z (2007) A modern odyssey on the ancient trade route. *China and the World Cultural Exchange*, **4**, 34–36.

This paper is a part of Zhijin Liu's PhD dissertation research, in which he uses field and laboratory-based approaches to examine the conservation status and population genetics of Yunnan snub-nosed Monkey. Ming Li, the corresponding author, participates in several international and national scientific projects concerning conservation biology, population genetics, landscape genetics and molecular evolution of Primates in China. Authors of this paper are involved in the Key Laboratory of Animal Ecology and Conservation Biology, Institute of Zoology, Chinese Academy of Sciences, which are leading by Professor Fuwen Wei now and focus on the behavioral and population ecology, conservation genetics, and molecular systematics in mammals and other vertebrates.

Supporting information

Additional supporting information may be found in the online version of this article.

Fig. S1 This figure illustrates the distribution of Q for each genetic cluster among individuals. The values of Q have been ranked. Also shown are lines giving the 95% posterior probability intervals for each individual.

Table S1 Summary of the goals and parameter sets of the different Structure runs

Table S2 Summary of the goals and parameter sets of the different GENELAND runs

Table S3 Summary of the parameter sets and results of the different im runs

Table S4 Number of alleles across samples (N_a), observed (H_O) and expected (H_E) heterozygosities and departures from Hardy–Weinberg proportions (F_{IS}) for all samples and for all loci

Please note: Wiley-Blackwell is not responsible for the content or functionality of any supporting information supplied by the authors. Any queries (other than missing material) should be directed to the corresponding author for the article.